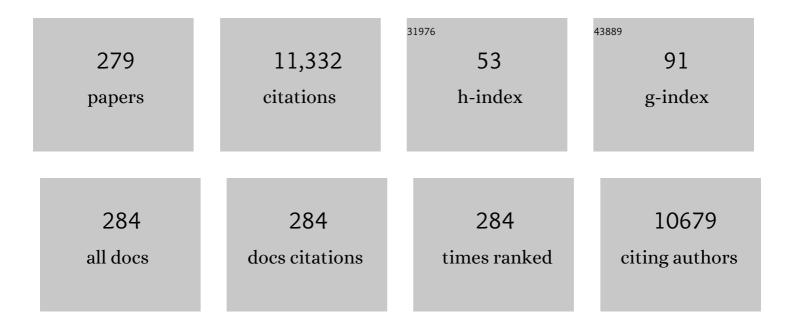
List of Publications by Year in descending order

Source: https://exaly.com/author-pdf/3654022/publications.pdf Version: 2024-02-01



LINDINGLI

#	Article	IF	CITATIONS
1	Ethane/ethylene separation in a metal-organic framework with iron-peroxo sites. Science, 2018, 362, 443-446.	12.6	763
2	Molecular sieving of ethylene from ethane using a rigid metal–organic framework. Nature Materials, 2018, 17, 1128-1133.	27.5	532
3	Synthesis of ZIFâ€8 and ZIFâ€67 by Steamâ€Assisted Conversion and an Investigation of Their Tribological Behaviors. Angewandte Chemie - International Edition, 2011, 50, 672-675.	13.8	382
4	A novel method for the preparation of zeolite ZSM-5. Journal of the Chemical Society Chemical Communications, 1990, , 755.	2.0	333
5	Flexible–Robust Metal–Organic Framework for Efficient Removal of Propyne from Propylene. Journal of the American Chemical Society, 2017, 139, 7733-7736.	13.7	242
6	Synthesis and hydrogen-storage behavior of metal–organic framework MOF-5. International Journal of Hydrogen Energy, 2009, 34, 1377-1382.	7.1	219
7	Hydrogen storage in several microporous zeolites. International Journal of Hydrogen Energy, 2007, 32, 4998-5004.	7.1	193
8	Covalent Triazine-Based Frameworks with Ultramicropores and High Nitrogen Contents for Highly Selective CO ₂ Capture. Environmental Science & Technology, 2016, 50, 4869-4876.	10.0	173
9	Coupling of Cu(100) and (110) Facets Promotes Carbon Dioxide Conversion to Hydrocarbons and Alcohols. Angewandte Chemie - International Edition, 2021, 60, 4879-4885.	13.8	171
10	Applications of metal–organic frameworks for green energy and environment: New advances in adsorptive gas separation, storage and removal. Green Energy and Environment, 2018, 3, 191-228.	8.7	158
11	Amorphous NiFeB nanoparticles realizing highly active and stable oxygen evolving reaction for water splitting. Nano Research, 2018, 11, 1664-1675.	10.4	129
12	Synthesis of metal–organic framework MIL-101 in TMAOH-Cr(NO3)3-H2BDC-H2O and its hydrogen-storage behavior. Microporous and Mesoporous Materials, 2010, 130, 174-179.	4.4	127
13	A Metal–Organic Framework with Suitable Pore Size and Specific Functional Sites for the Removal of Trace Propyne from Propylene. Angewandte Chemie - International Edition, 2018, 57, 15183-15188.	13.8	124
14	Oxygen vacancies engineered self-supported B doped Co3O4 nanowires as an efficient multifunctional catalyst for electrochemical water splitting and hydrolysis of sodium borohydride. Chemical Engineering Journal, 2021, 404, 126474.	12.7	122
15	Two-Dimensional Covalent Triazine Framework Membrane for Helium Separation and Hydrogen Purification. ACS Applied Materials & Interfaces, 2016, 8, 8694-8701.	8.0	121
16	Fabrication of mesoporous NiFe2O4 nanorods as efficient oxygen evolution catalyst for water splitting. Electrochimica Acta, 2016, 211, 871-878.	5.2	117
17	Adsorption of CO ₂ , CH ₄ , and N ₂ on 8-, 10-, and 12-Membered Ring Hydrophobic Microporous High-Silica Zeolites: DDR, Silicalite-1, and Beta. Industrial & Engineering Chemistry Research, 2013, 52, 17856-17864.	3.7	114
18	Theoretical Expectation and Experimental Implementation of In Situ Al-Doped CoS ₂ Nanowires on Dealloying-Derived Nanoporous Intermetallic Substrate as an Efficient Electrocatalyst for Boosting Hydrogen Production. ACS Catalysis, 2019, 9, 1489-1502.	11.2	112

#	Article	IF	CITATIONS
19	A Copper(II)-Paddlewheel Metal–Organic Framework with Exceptional Hydrolytic Stability and Selective Adsorption and Detection Ability of Aniline in Water. ACS Applied Materials & Interfaces, 2017, 9, 27027-27035.	8.0	109
20	Three-dimensional well-mixed / highly-densed NiS-CoS nanorod arrays: An efficient and stable bifunctional electrocatalyst for hydrogen and oxygen evolution reactions. Electrochimica Acta, 2018, 260, 82-91.	5.2	109
21	Kinetic separation of propylene over propane in a microporous metal-organic framework. Chemical Engineering Journal, 2018, 354, 977-982.	12.7	108
22	Uniformly mesoporous NiO/NiFe2O4 biphasic nanorods as efficient oxygen evolving catalyst for water splitting. International Journal of Hydrogen Energy, 2016, 41, 17976-17986.	7.1	106
23	Separation of CO 2 /CH 4 and CH 4 /N 2 mixtures by M/DOBDC: A detailed dynamic comparison with MIL-100(Cr) and activated carbon. Microporous and Mesoporous Materials, 2014, 198, 236-246.	4.4	105
24	3D porous network heterostructure NiCe@NiFe electrocatalyst for efficient oxygen evolution reaction at large current densities. Applied Catalysis B: Environmental, 2020, 260, 118199.	20.2	100
25	Improved 2,3-butanediol production from corncob acid hydrolysate by fed-batch fermentation using Klebsiella oxytoca. Process Biochemistry, 2010, 45, 613-616.	3.7	99
26	A Metal–Organic Framework with Suitable Pore Size and Specific Functional Sites for the Removal of Trace Propyne from Propylene. Angewandte Chemie, 2018, 130, 15403-15408.	2.0	98
27	Mixed-matrix membranes based on Zn/Ni-ZIF-8-PEBA for high performance CO2 separation. Journal of Membrane Science, 2018, 560, 38-46.	8.2	97
28	Synthesis and hydrogen storage studies of metalâ^'organic framework UiO-66. International Journal of Hydrogen Energy, 2013, 38, 13104-13109.	7.1	91
29	Ionothermal Synthesis of Zirconium Phosphates and Their Catalytic Behavior in the Selective Oxidation of Cyclohexane. Angewandte Chemie - International Edition, 2009, 48, 2206-2209.	13.8	89
30	Efficient separation of ethylene from acetylene/ethylene mixtures by a flexible-robust metal–organic framework. Journal of Materials Chemistry A, 2017, 5, 18984-18988.	10.3	88
31	Highly Adsorptive Separation of Ethane/Ethylene by An Ethane-Selective MOF MIL-142A. Industrial & Engineering Chemistry Research, 2018, 57, 4063-4069.	3.7	88
32	Guest-dependent pressure induced gate-opening effect enables effective separation of propene and propane in a flexible MOF. Chemical Engineering Journal, 2018, 346, 489-496.	12.7	87
33	Adsorption of CO ₂ , CH ₄ , and N ₂ on Gas Diameter Grade Ion-Exchange Small Pore Zeolites. Journal of Chemical & Engineering Data, 2012, 57, 3701-3709.	1.9	85
34	Self-Supported Ternary Ni–S–Se Nanorod Arrays as Highly Active Electrocatalyst for Hydrogen Generation in Both Acidic and Basic Media: Experimental Investigation and DFT Calculation. ACS Applied Materials & Interfaces, 2018, 10, 2430-2441.	8.0	83
35	Exploiting the gate opening effect in a flexible MOF for selective adsorption of propyne from C1/C2/C3 hydrocarbons. Journal of Materials Chemistry A, 2016, 4, 751-755.	10.3	81
36	Theoretical investigation of gas separation in functionalized nanoporous graphene membranes. Applied Surface Science, 2017, 407, 532-539.	6.1	80

#	Article	IF	CITATIONS
37	A Strategy for Constructing Pore‧paceâ€Partitioned MOFs with High Uptake Capacity for C ₂ Hydrocarbons and CO ₂ . Angewandte Chemie - International Edition, 2020, 59, 19027-19030.	13.8	77
38	Encapsulation of Ni/Fe ₃ O ₄ heterostructures inside onion-like N-doped carbon nanorods enables synergistic electrocatalysis for water oxidation. Nanoscale, 2018, 10, 3997-4003.	5.6	75
39	Facile fabrication of robust 3D Fe–NiSe nanowires supported on nickel foam as a highly efficient, durable oxygen evolution catalyst. Journal of Materials Chemistry A, 2017, 5, 14639-14645.	10.3	74
40	A Tale of Two Trimers from Two Different Worlds: A COFâ€Inspired Synthetic Strategy for Poreâ€Space Partitioning of MOFs. Angewandte Chemie - International Edition, 2019, 58, 6316-6320.	13.8	70
41	Robust Microporous Metal–Organic Frameworks for Highly Efficient and Simultaneous Removal of Propyne and Propadiene from Propylene. Angewandte Chemie - International Edition, 2019, 58, 10209-10214.	13.8	69
42	Loading FeOOH on Ni(OH) ₂ hollow nanorods to obtain a three-dimensional sandwich catalyst with strong electron interactions for an efficient oxygen evolution reaction. Nanoscale, 2020, 12, 983-990.	5.6	69
43	One-step solid-phase boronation to fabricate self-supported porous FeNiB/FeNi foam for efficient electrocatalytic oxygen evolution and overall water splitting. Journal of Materials Chemistry A, 2019, 7, 19554-19564.	10.3	68
44	lonothermal Synthesis and Structure Analysis of an Openâ€Framework Zirconium Phosphate with a High CO ₂ /CH ₄ Adsorption Ratio. Angewandte Chemie - International Edition, 2011, 50, 8139-8142.	13.8	67
45	Solvent effect on the synthesis of MIL-96(Cr) and MIL-100(Cr). Microporous and Mesoporous Materials, 2011, 142, 489-493.	4.4	66
46	A novel silver oxides oxygen evolving catalyst for water splitting. International Journal of Hydrogen Energy, 2011, 36, 7374-7380.	7.1	63
47	Mixed-metal MOF-derived Co-doped Ni3C/Ni NPs embedded in carbon matrix as an efficient electrocatalyst for oxygen evolution reaction. International Journal of Hydrogen Energy, 2019, 44, 24572-24579.	7.1	63
48	Nanostructured NiFe (oxy)hydroxide with easily oxidized Ni towards efficient oxygen evolution reactions. Journal of Materials Chemistry A, 2018, 6, 16810-16817.	10.3	61
49	Porous Niâ^'Moâ^'S Nanowire Network Film Electrode as a Highâ€Efficiency Bifunctional Electrocatalyst for Overall Water Splitting. ChemElectroChem, 2018, 5, 335-342.	3.4	60
50	IrO2 nanoparticle-decorated single-layer NiFe LDHs nanosheets with oxygen vacancies for the oxygen evolution reaction. Chemical Engineering Journal, 2020, 399, 125738.	12.7	60
51	Facile and fast fabrication of iron-phosphate supported on nickel foam as a highly efficient and stable oxygen evolution catalyst. Journal of Materials Chemistry A, 2017, 5, 18627-18633.	10.3	59
52	Mesoporous nickel–iron binary oxide nanorods for efficient electrocatalytic water oxidation. Nano Research, 2017, 10, 2096-2105.	10.4	57
53	Size-controlled synthesis of SnO2 quantum dots and their gas-sensing performance. Applied Surface Science, 2015, 346, 256-262.	6.1	56
54	Realizing high performance solar water oxidation for Ti-doped hematite nanoarrays by synergistic decoration with ultrathin cobalt-iron phosphate nanolayers. Chemical Engineering Journal, 2019, 355, 49-57.	12.7	56

#	Article	IF	CITATIONS
55	Exploration of nanoporous graphene membranes for the separation of N ₂ from CO ₂ : a multi-scale computational study. Physical Chemistry Chemical Physics, 2016, 18, 8352-8358.	2.8	55
56	Polyvinylamine/graphene oxide/PANI@CNTs mixed matrix composite membranes with enhanced CO2/N2 separation performance. Journal of Membrane Science, 2019, 589, 117246.	8.2	54
57	Recyclable ammonia uptake of a MIL series of metal-organic frameworks with high structural stability. Microporous and Mesoporous Materials, 2018, 258, 170-177.	4.4	52
58	lonothermal synthesis of a three-dimensional zinc phosphate with DFT topology using unstable deep-eutectic solvent as template-delivery agent. Microporous and Mesoporous Materials, 2008, 115, 624-628.	4.4	51
59	Environmentally friendly synthesis of flexible MOFs M(NA) ₂ (M = Zn, Co, Cu, Cd) with large and regenerable ammonia capacity. Journal of Materials Chemistry A, 2018, 6, 9922-9929.	10.3	51
60	Zeolite CAN and AFI-Type Zeolitic Imidazolate Frameworks with Large 12-Membered Ring Pore Openings Synthesized Using Bulky Amides as Structure-Directing Agents. Journal of the American Chemical Society, 2016, 138, 16232-16235.	13.7	50
61	Ultrasmall NiFe-Phosphate Nanoparticles Incorporated α-Fe ₂ O ₃ Nanoarrays Photoanode Realizing High Efficient Solar Water Splitting. ACS Sustainable Chemistry and Engineering, 2018, 6, 2353-2361.	6.7	50
62	Methane-trapping metal–organic frameworks with an aliphatic ligand for efficient CH ₄ /N ₂ separation. Sustainable Energy and Fuels, 2020, 4, 138-142.	4.9	50
63	Experimental and simulation study on efficient CH4/N2 separation by pressure swing adsorption on silicalite-1 pellets. Chemical Engineering Journal, 2020, 388, 124222.	12.7	50
64	Pore-Space Partition and Optimization for Propane-Selective High-Performance Propane/Propylene Separation. ACS Applied Materials & amp; Interfaces, 2021, 13, 52160-52166.	8.0	50
65	Integrated production of xylitol and ethanol using corncob. Applied Microbiology and Biotechnology, 2010, 87, 411-417.	3.6	48
66	Selective Adsorptive Separation of CO ₂ /CH ₄ and CO ₂ /N ₂ by a Water Resistant Zirconium–Porphyrin Metal–Organic Framework. Industrial & Engineering Chemistry Research, 2018, 57, 12215-12224.	3.7	48
67	Opportunities and critical factors of porous metal–organic frameworks for industrial light olefins separation. Materials Chemistry Frontiers, 2020, 4, 1954-1984.	5.9	48
68	La-RuO2 nanocrystals with efficient electrocatalytic activity for overall water splitting in acidic media: Synergistic effect of La doping and oxygen vacancy. Chemical Engineering Journal, 2022, 439, 135699.	12.7	47
69	Amorphous CoFeBO nanoparticles as highly active electrocatalysts for efficient water oxidation reaction. International Journal of Hydrogen Energy, 2018, 43, 6138-6149.	7.1	46
70	Ionothermal Synthesis of Layered Zirconium Phosphates and Their Tribological Properties in Mineral Oil. Inorganic Chemistry, 2010, 49, 8270-8275.	4.0	44
71	Separation of CO2/CH4 and CH4/N2 mixtures using MOF-5 and Cu3(BTC)2. Journal of Energy Chemistry, 2014, 23, 453-460.	12.9	42
72	Flexible Metal–Organic Frameworks with Discriminatory Gateâ€Opening Effect for the Separation of Acetylene from Ethylene/Acetylene Mixtures. European Journal of Inorganic Chemistry, 2016, 2016, 4457-4462.	2.0	42

#	Article	IF	CITATIONS
73	Facile synthesis, characterization and DFT studies of a nanostructured nickel–molybdenum–phosphorous planar electrode as an active electrocatalyst for the hydrogen evolution reaction. Nanoscale, 2019, 11, 9353-9361.	5.6	42
74	Amorphous iron-nickel phosphide nanocone arrays as efficient bifunctional electrodes for overall water splitting. Green Energy and Environment, 2021, 6, 496-505.	8.7	42
75	Highly efficient Ni nanotube arrays and Ni nanotube arrays coupled with NiFe layered-double-hydroxide electrocatalysts for overall water splitting. Journal of Power Sources, 2020, 448, 227434.	7.8	41
76	Self-Assembly of Gridlike Zinc Oxide Lamellae for Chemical-Sensing Applications. ACS Applied Materials & amp; Interfaces, 2015, 7, 5870-5878.	8.0	40
77	Enhancing the water oxidation activity of Ni2P nanocatalysts by iron-doping and electrochemical activation. Electrochimica Acta, 2017, 253, 498-505.	5.2	40
78	Ammonia capture and flexible transformation of M-2(INA) (M = Cu, Co, Ni, Cd) series materials. Journal of Hazardous Materials, 2016, 306, 340-347.	12.4	39
79	MIL-100Cr with open Cr sites for a record N ₂ O capture. Chemical Communications, 2018, 54, 14061-14064.	4.1	39
80	Adsorption CO2, CH4 and N2 on two different spacing flexible layer MOFs. Microporous and Mesoporous Materials, 2012, 161, 154-159.	4.4	37
81	Adsorption and separation of CO2 on Fe(II)-MOF-74: Effect of the open metal coordination site. Journal of Solid State Chemistry, 2014, 213, 224-228.	2.9	36
82	Enhancement of hydrogen desorption in magnesium hydride catalyzed by graphene nanosheets supported Ni-CeOx hybrid nanocatalyst. International Journal of Hydrogen Energy, 2016, 41, 10786-10794.	7.1	36
83	Regulating the Sensitivity and Operating Temperatures by Morphology Engineering of 2D ZnO Nanostructures and 3D ZnO Microstructures for the Detection of Organic-Amines. ACS Applied Nano Materials, 2019, 2, 5430-5439.	5.0	36
84	Highly Effective Ru/BaCeO ₃ Catalysts on Supports with Strong Basic Sites for Ammonia Synthesis. Chemistry - an Asian Journal, 2019, 14, 2815-2821.	3.3	36
85	Effective CH4 enrichment from N2 by SIM-1 via a strong adsorption potential SOD cage. Separation and Purification Technology, 2020, 230, 115850.	7.9	36
86	Microporous metal-organic framework with specific functional sites for efficient removal of ethane from ethane/ethylene mixtures. Chemical Engineering Journal, 2020, 387, 124137.	12.7	36
87	The effects of ceria morphology on the properties of Pd/ceria catalyst for catalytic oxidation of low-concentration methane. Journal of Materials Science, 2016, 51, 10917-10925.	3.7	35
88	Kinetically controlled ammonia vapor diffusion synthesis of a Zn(<scp>ii</scp>) MOF and its H ₂ O/NH ₃ adsorption properties. Journal of Materials Chemistry A, 2016, 4, 10345-10351.	10.3	35
89	Microregulation of Pore Channels in Covalent-Organic Frameworks Used for the Selective and Efficient Separation of Ethane. ACS Applied Materials & Interfaces, 2020, 12, 52819-52825.	8.0	35
90	Experiments and simulations on separating a CO2/CH4 mixture using K-KFI at low and high pressures. Microporous and Mesoporous Materials, 2014, 184, 21-27.	4.4	34

#	Article	IF	CITATIONS
91	Removal of Ammonia Emissions via Reversible Structural Transformation in M(BDC) (M = Cu, Zn, Cd) Metal–Organic Frameworks. Environmental Science & Technology, 2020, 54, 3636-3642.	10.0	34
92	Tuning the Pore Environment of MOFs toward Efficient CH ₄ /N ₂ Separation under Humid Conditions. ACS Applied Materials & Interfaces, 2022, 14, 15830-15839.	8.0	34
93	Protection of open-metal V(III) sites and their associated CO2/CH4/N2/O2/H2O adsorption properties in mesoporous V-MOFs. Journal of Colloid and Interface Science, 2015, 456, 197-205.	9.4	33
94	Hierarchical porous carbons derived from microporous zeolitic metal azolate frameworks for supercapacitor electrodes. Materials Research Bulletin, 2017, 88, 62-68.	5.2	32
95	Enhancing the CO2 separation performance of SPEEK membranes by incorporation of polyaniline-decorated halloysite nanotubes. Journal of Membrane Science, 2019, 573, 602-611.	8.2	32
96	Synergistic Assembly of a CoS@NiFe/Ni Foam Heterostructure Electrocatalyst for Efficient Water Oxidation Catalysis at Large Current Densities. Chemistry - an Asian Journal, 2020, 15, 1484-1492.	3.3	32
97	Down-sizing the crystal size of ZK-5 zeolite for its enhanced CH4 adsorption and CH4/N2 separation performances. Chemical Engineering Journal, 2021, 406, 126599.	12.7	32
98	Morphology Effect of Ceria on the Ammonia Synthesis Activity of Ru/CeO2 Catalysts. Catalysis Letters, 2019, 149, 1007-1016.	2.6	31
99	Mesoporous Co3O4 derived from Co-MOFs with different morphologies and ligands for toluene catalytic oxidation. Chemical Engineering Science, 2020, 220, 115654.	3.8	31
100	Modification of the pore environment in UiO-type metal-organic framework toward boosting the separation of propane/propylene. Chemical Engineering Journal, 2021, 403, 126428.	12.7	31
101	Targeted capture and pressure/temperature-responsive separation in flexible metal–organic frameworks. Journal of Materials Chemistry A, 2015, 3, 22574-22583.	10.3	30
102	Well-dispersed palladium nanoparticles on nickel- phosphorus nanosheets as efficient three-dimensional platform for superior catalytic glucose electro-oxidation and non-enzymatic sensing. Journal of Colloid and Interface Science, 2018, 511, 355-364.	9.4	30
103	Amorphous CoFeP/NC hybrids as highly efficient electrocatalysts for water oxidation. International Journal of Hydrogen Energy, 2019, 44, 30196-30207.	7.1	30
104	Optimized pore environment for efficient high selective C2H2/C2H4 and C2H2/CO2 separation in a metal-organic framework. Separation and Purification Technology, 2021, 256, 117749.	7.9	30
105	Highly catalytic flexible RuO2 on carbon fiber cloth network for boosting chlorine evolution reaction. Electrochimica Acta, 2019, 307, 385-392.	5.2	29
106	Hybrid Ni ₃ S ₂ –MoS ₂ nanowire arrays as a pH-universal catalyst for accelerating the hydrogen evolution reaction. Chemical Communications, 2020, 56, 2471-2474.	4.1	29
107	Strengthen metal-oxygen covalency of CoFe-layered double hydroxide for efficient mild oxygen evolution. Nano Research, 2022, 15, 162-169.	10.4	29
108	Exploiting the pore size and functionalization effects in UiO topology structures for the separation of light hydrocarbons. CrystEngComm, 2017, 19, 1729-1737.	2.6	28

#	Article	IF	CITATIONS
109	Highly sensitive and selective gas-phase ethanolamine sensor by doping sulfur into nanostructured ZnO. Sensors and Actuators B: Chemical, 2019, 296, 126633.	7.8	28
110	Construction of saturated coordination titanium-based metal–organic framework for one-step C2H2/C2H6/C2H4 separation. Separation and Purification Technology, 2021, 276, 119284.	7.9	28
111	Controllable synthesis of prism- and lamella-like ZnO and their gas sensing. Materials Letters, 2014, 136, 427-430.	2.6	27
112	Insight into the effect of surface structure on H2 adsorption and activation over different CuO(1 1 1) surfaces: A first-principle study. Computational Materials Science, 2016, 122, 191-200.	3.0	27
113	Fabrication of Fe-doped Co2P nanoparticles as efficient electrocatalyst for electrochemical and photoelectrochemical water oxidation. Electrochimica Acta, 2018, 283, 1490-1497.	5.2	27
114	Ethylenediamine-functionalized metal organic frameworks MIL-100(Cr) for efficient CO2/N2O separation. Separation and Purification Technology, 2020, 235, 116219.	7.9	27
115	Simple self-assembly of 3D laminated CuO/SnO2 hybrid for the detection of triethylamine. Chinese Chemical Letters, 2020, 31, 2055-2058.	9.0	27
116	Antenna-Protected Metal–Organic Squares for Water/Ammonia Uptake with Excellent Stability and Regenerability. ACS Sustainable Chemistry and Engineering, 2017, 5, 5082-5089.	6.7	26
117	Enhanced mass transfer on hierarchical porous pure silica zeolite used for gas separation. Microporous and Mesoporous Materials, 2018, 266, 56-63.	4.4	26
118	Porous versus Compact Hematite Nanorod Photoanode for High-Performance Photoelectrochemical Water Oxidation. ACS Sustainable Chemistry and Engineering, 2019, 7, 11377-11385.	6.7	26
119	BiVO4 photoanode decorated with cobalt-manganese layered double hydroxides for enhanced photoelectrochemical water oxidation. International Journal of Hydrogen Energy, 2020, 45, 31902-31912.	7.1	26
120	A Strategy for Constructing Poreâ€Spaceâ€Partitioned MOFs with High Uptake Capacity for C 2 Hydrocarbons and CO 2. Angewandte Chemie, 2020, 132, 19189-19192.	2.0	26
121	Polyvinylamine/amorphous metakaolin mixed-matrix composite membranes with facilitated transport carriers for highly efficient CO2/N2 separation. Journal of Membrane Science, 2020, 599, 117828.	8.2	26
122	Highly Dispersed Mo ₂ C Nanodots in Carbon Nanocages Derived from Moâ€Based Xerogel: Efficient Electrocatalysts for Hydrogen Evolution. Small Methods, 2021, 5, e2100334.	8.6	26
123	Three-dimensional self-supporting catalyst with NiFe alloy/oxyhydroxide supported on high-surface cobalt hydroxide nanosheet array for overall water splitting. Journal of Colloid and Interface Science, 2022, 606, 873-883.	9.4	26
124	Structure and kinetic investigations of surface-stepped CeO 2 -supported Pd catalysts for low-concentration methane oxidation. Chemical Engineering Journal, 2016, 306, 745-753.	12.7	25
125	Ti-doped hematite photoanode with surface phosphate ions functionalization for synergistic enhanced photoelectrochemical water oxidation. Electrochimica Acta, 2019, 307, 197-205.	5.2	25
126	Self‣upported 3 D Ultrathin Cobalt–Nickel–Boron Nanoflakes as an Efficient Electrocatalyst for the Oxygen Evolution Reaction. ChemSusChem, 2020, 13, 3662-3670.	6.8	25

#	Article	IF	CITATIONS
127	Computational study of oxygen adsorption in metal–organic frameworks with exposed cation sites: effect of framework metal ions. RSC Advances, 2015, 5, 33432-33437.	3.6	24
128	Graphene-like Poly(triazine imide) as N ₂ -Selective Ultrathin Membrane for Postcombustion CO ₂ Capture. Journal of Physical Chemistry C, 2016, 120, 28782-28788.	3.1	24
129	(CH ₃) ₂ NHâ€Assisted Synthesis of Highâ€Purity Niâ€HKUSTâ€1 for the Adsorption of CO ₂ , CH ₄ , and N ₂ . European Journal of Inorganic Chemistry, 2018, 2018, 1047-1052.	2.0	24
130	Mixed-matrix membranes consisting of Pebax and novel nitrogen-doped porous carbons for CO2 separation. Journal of Membrane Science, 2022, 644, 120182.	8.2	24
131	A WO3/Ag–Bi oxygen-evolution catalyst for splitting water under mild conditions. International Journal of Hydrogen Energy, 2012, 37, 13249-13255.	7.1	23
132	Preparation of nanostructured mesoporous NiCo2O4 and its electrocatalytic activities for water oxidation. Journal of Energy Chemistry, 2015, 24, 271-277.	12.9	23
133	CH4/N2 separation on methane molecules grade diameter channel molecular sieves with a CHA-type structure. Chinese Journal of Chemical Engineering, 2019, 27, 1044-1049.	3.5	23
134	Mesoporous Co ₃ O ₄ Derived from Facile Calcination of Octahedral Co-MOFs for Toluene Catalytic Oxidation. Industrial & Engineering Chemistry Research, 2020, 59, 5583-5590.	3.7	23
135	Preparation, Characterization, and Catalytical Application of MgCoAl-Hydrotalcite-Like Compounds. Journal of Natural Gas Chemistry, 2007, 16, 371-376.	1.8	22
136	Template control in ionothermal synthesis of aluminophosphate microporous materials. Dalton Transactions, 2009, , 10418.	3.3	22
137	Catalytic performance of Mo ₂ C supported on onion-like carbon for dehydrogenation of cyclohexane. RSC Advances, 2014, 4, 53950-53953.	3.6	22
138	CO2/CH4 and CH4/N2 separation on isomeric metal organic frameworks. Chinese Journal of Chemical Engineering, 2016, 24, 1687-1694.	3.5	22
139	Polyvinylamine/ZIF-8-decorated metakaolin composite membranes for CO2/N2 separation. Separation and Purification Technology, 2021, 270, 118800.	7.9	22
140	S-Doped three-dimensional graphene (S-3DG): a metal-free electrocatalyst for the electrochemical synthesis of ammonia under ambient conditions. Dalton Transactions, 2020, 49, 2258-2263.	3.3	20
141	Preparation of a Bimetallic NiFeâ€MOF on Nickel Foam as a Highly Efficient Electrocatalyst for Oxygen Evolution Reaction. ChemistrySelect, 2021, 6, 1320-1327.	1.5	20
142	A stable metal–organic framework with wellâ€matched pore cavity for efficient acetylene separation. AICHE Journal, 2021, 67, e17152.	3.6	20
143	Synthesis, characterization and crystal structure analysis of an open-framework zirconium phosphate. Microporous and Mesoporous Materials, 2007, 104, 185-191.	4.4	19
144	A crystal seeds-assisted synthesis of microporous and mesoporous silicalite-1 and their CO 2 /N 2 /CH 4 /C 2 H 6 adsorption properties. Microporous and Mesoporous Materials, 2017, 242, 231-237.	4.4	19

#	Article	IF	CITATIONS
145	Reversed ethane/ethylene adsorption in a metal–organic framework via introduction of oxygen. Chinese Journal of Chemical Engineering, 2020, 28, 593-597.	3.5	19
146	Synthesis of metal-organic frameworks from the system metal/ <scp>L</scp> -glutamic acid/TEA/H ₂ O. Journal of Coordination Chemistry, 2009, 62, 1959-1963.	2.2	18
147	Improved synthesis and hydrogen storage of a microporous metal–organic framework material. Energy Conversion and Management, 2009, 50, 1314-1317.	9.2	18
148	Mesoporous Co ₃ O ₄ @carbon composites derived from microporous cobalt-based porous coordination polymers for enhanced electrochemical properties in supercapacitors. RSC Advances, 2016, 6, 18465-18470.	3.6	18
149	Adjusting the proportions of extra-framework K+ and Cs+ cations to construct a "molecular gate―on ZK-5 for CO2 removal. Microporous and Mesoporous Materials, 2018, 268, 50-57.	4.4	18
150	Hollow Hemispherical Carbon Microspheres with Mo ₂ C Nanoparticles Synthesized by Precursor Design: Effective Noble Metalâ€Free Catalysts for Dehydrogenation. Small Methods, 2020, 4, 1900597.	8.6	18
151	Ultrafine Mo ₂ C Nanoparticles Confined in 2D Meshlike Carbon Nanolayers for Effective Hydrogen Evolution. ChemCatChem, 2020, 12, 3195-3201.	3.7	18
152	N, S synergistic effect in hierarchical porous carbon for enhanced NRR performance. Carbon, 2021, 179, 358-364.	10.3	18
153	Construction of a Porous Metal–Organic Framework with a High Density of Open Cr Sites for Record N ₂ /O ₂ Separation. Advanced Materials, 2021, 33, e2100866.	21.0	18
154	Effects of different alkali metal cations in FAU zeolites on the separation performance of CO2/N2O. Chemical Engineering Journal, 2022, 431, 134257.	12.7	18
155	Substituent-Induced Electron-Transfer Strategy for Selective Adsorption of N ₂ in MIL-101(Cr)-X Metal–Organic Frameworks. ACS Applied Materials & Interfaces, 2022, 14, 2146-2154.	8.0	18
156	Enhancing CO2 separation performance of mixed matrix membranes by incorporation of L-cysteine-functionalized MoS2. Separation and Purification Technology, 2022, 297, 121560.	7.9	18
157	Cu2-xSe@CuO core-shell assembly grew on copper foam for efficient oxygen evolution. International Journal of Hydrogen Energy, 2019, 44, 31979-31986.	7.1	17
158	High performance for oxidation of low-concentration methane using ultra-low Pd in silicalite-1 zeolite. Microporous and Mesoporous Materials, 2019, 284, 235-240.	4.4	17
159	A facile controllable self-assembly of 3D elliptical ZnO microspheres from 1D nanowires for effective detection of acetone. Materials Letters, 2020, 270, 127706.	2.6	17
160	Direct Functionalization of the Open Metal Sites in Rare Earth-Based Metal–Organic Frameworks Used for the Efficient Separation of Ethylene. Industrial & Engineering Chemistry Research, 2020, 59, 6123-6129.	3.7	17
161	Morphology evolution of ZnO by controlling solvent and electrochemical sensing of hexagonal nanotablets toward amines. Chinese Chemical Letters, 2020, 31, 2091-2094.	9.0	17
162	Design and Synthesis Strategies: 2D Materials for Electromagnetic Shielding/Absorbing. Chemistry - an Asian Journal, 2021, 16, 3817-3832.	3.3	17

#	Article	IF	CITATIONS
163	Mo-chelate strategy for synthesizing ultrasmall Mo2C nanoparticles embedded in carbon nanosheets for efficient hydrogen evolution. International Journal of Hydrogen Energy, 2021, 46, 31598-31607.	7.1	17
164	Acid-treatment-assisted synthesis of Pt–Sn/graphene catalysts and their enhanced ethanol electro-catalytic activity. International Journal of Hydrogen Energy, 2015, 40, 990-997.	7.1	16
165	Novel copper oxides oxygen evolving catalyst in situ for electrocatalytic water splitting. Electrochimica Acta, 2015, 152, 280-285.	5.2	16
166	Vapor phase solvents loaded in zeolite as the sustainable medium for the preparation of Cu-BTC and ZIF-8. Chemical Engineering Journal, 2017, 313, 179-186.	12.7	16
167	Robust Microporous Metal–Organic Frameworks for Highly Efficient and Simultaneous Removal of Propyne and Propadiene from Propylene. Angewandte Chemie, 2019, 131, 10315-10320.	2.0	16
168	Preparation of a Dualâ€MOF Heterostructure (ZIF@MIL) for Enhanced Oxygen Evolution Reaction Activity. Chemistry - an Asian Journal, 2021, 16, 64-71.	3.3	16
169	An ethane-favored metal-organic framework with tailored pore environment used for efficient ethylene separation. Microporous and Mesoporous Materials, 2021, 320, 111096.	4.4	16
170	Metal-Ci oxygen-evolving catalysts generated in situ in a mild H2O/CO2 environment. International Journal of Hydrogen Energy, 2013, 38, 5251-5258.	7.1	15
171	A mild H3BO3 environment for water splitting. International Journal of Hydrogen Energy, 2013, 38, 10191-10195.	7.1	15
172	Poly (triazine imide) (PTI) and graphene hybrids supported Pt Sn catalysts for enhanced electrocatalytic oxidation of ethanol. Applied Surface Science, 2019, 492, 879-885.	6.1	15
173	The Pd/Na-ZSM-5 catalysts with different Si/Al ratios on low concentration methane oxidation. Solid State Sciences, 2020, 101, 106097.	3.2	15
174	Research on CO2-N2O separation using flexible metal organic frameworks. Separation and Purification Technology, 2020, 251, 117311.	7.9	15
175	SPEEK membranes by incorporation of NaY zeolite for CO2/N2 separation. Separation and Purification Technology, 2021, 275, 119189.	7.9	15
176	Novel zeolite/carbon monolith adsorbents for efficient CH4/N2 separation. Chemical Engineering Journal, 2021, 426, 130163.	12.7	15
177	Review—Nanostructural ZnO-Based Electrochemical Sensor for Environmental Application. Journal of the Electrochemical Society, 2022, 169, 020573.	2.9	15
178	Synthesis, Structure, and Characterization of Two Photoluminescent Zirconium Phosphateâ^'Quinoline Compounds. Inorganic Chemistry, 2009, 48, 8947-8954.	4.0	14
179	Synthesis of α-layered sodium disilicate and its tribological properties in liquid paraffin. Journal of Materials Chemistry, 2009, 19, 6896.	6.7	14
180	Spatiotemporal Variability of Remotely Sensed PM2.5 Concentrations in China from 1998 to 2014 Based on a Bayesian Hierarchy Model. International Journal of Environmental Research and Public Health, 2016, 13, 772.	2.6	14

#	Article	IF	CITATIONS
181	Functionalized Metal–Organic Frameworks for the Efficient Removal of Low Concentrations of Ammonia. ChemPlusChem, 2016, 81, 222-228.	2.8	14
182	Efficient Catalysts for Cyclohexane Dehydrogenation Synthesized by Mo-Promoted Growth of 3D Block Carbon Coupled with Mo ₂ C. ACS Omega, 2018, 3, 10773-10780.	3.5	14
183	A Tale of Two Trimers from Two Different Worlds: A COFâ€Inspired Synthetic Strategy for Poreâ€Space Partitioning of MOFs. Angewandte Chemie, 2019, 131, 6382-6386.	2.0	14
184	2D feather-shaped alumina slice as efficient Pd catalyst support for oxidation reaction of the low-concentration methane. Chemical Engineering Journal, 2019, 361, 1345-1351.	12.7	14
185	Boosting molecular recognition of acetylene in UiO-66 framework through pore environment functionalization. Chemical Engineering Science, 2021, 237, 116572.	3.8	14
186	Rational introduction of S and P in multi-stage electrocatalyst to drive a large-current-density water oxidation reaction and overall water splitting. Journal of Power Sources, 2022, 518, 230757.	7.8	14
187	Biomass-derived carbon nanosheets coupled with MoO2/Mo2C electrocatalyst for hydrogen evolution reaction. International Journal of Hydrogen Energy, 2022, 47, 30959-30969.	7.1	14
188	Autogenous growth of highly active bifunctional Ni–Fe2B nanosheet arrays toward efficient overall water splitting. International Journal of Hydrogen Energy, 2022, 47, 8303-8313.	7.1	14
189	Modulated crystalline Ag-Ci oxygen-evolving catalysts for electrocatalytic water oxidation. International Journal of Hydrogen Energy, 2014, 39, 1364-1370.	7.1	13
190	Palladium catalyst supported on stair-like microstructural CeO 2 provides enhanced activity and stability for low-concentration methane oxidation. Applied Catalysis A: General, 2016, 524, 237-242.	4.3	13
191	Cucurbit[7]uril–tetraphenylethene host–guest system induced emission activity. RSC Advances, 2016, 6, 4478-4482.	3.6	13
192	Improved synthesis of trigone trimer cluster metal organic framework MIL-100Al by a later entry of methyl groups. Chemical Communications, 2016, 52, 725-728.	4.1	13
193	Phosphate ions-functionalized and wettability-tuned nickel ferrite for boosted oxygen evolution performance. International Journal of Hydrogen Energy, 2019, 44, 26992-27000.	7.1	13
194	Mesoporous Carbon Nanotablets Coupled with Mo 2 C Nanoparticles: Combining Morphology and Structure to Realize High Activity for Efficient Hydrogen Evolution. ChemistrySelect, 2020, 5, 5974-5980.	1.5	13
195	The efficient separation of N ₂ O/CO ₂ using unsaturated Fe ²⁺ sites in MIL-100Fe. Chemical Communications, 2021, 57, 6636-6639.	4.1	13
196	Synthesis of Ultrathin and Gridâ€Structural Carbon Nanosheets Coupled with Mo ₂ C for Electrocatalytic Hydrogen Production. Chemistry - an Asian Journal, 2021, 16, 2107-2112.	3.3	13
197	Bimetallic Cuâ^'Coâ^'Se Nanotube Arrays Assembled on 3D Framework: an Efficient Bifunctional Electrocatalyst for Overall Water Splitting. ChemSusChem, 2021, 14, 5065-5074.	6.8	13
198	Concentrating and activating carbon dioxide over AuCu aerogel grain boundaries. Journal of Chemical Physics, 2020, 152, 204703.	3.0	13

#	Article	IF	CITATIONS
199	Efficient N2/CH4 separation in a stable metal–organic framework with high density of open Cr sites. Separation and Purification Technology, 2022, 281, 119951.	7.9	13
200	Different effect of Y (YÂ=ÂCu, Mn, Fe, Ni) doping on Co3O4 derived from Co-MOF for toluene catalytic destruction. Chemical Engineering Science, 2022, 251, 117436.	3.8	13
201	Synthesis of large single crystals of a clathrate compound MTN (a zeolite-like material) by the vapor-phase method. Materials Letters, 2008, 62, 4-6.	2.6	12
202	Adsorption and molecular simulation of CO2 and CH4 in two-dimensional metal–organic frameworks with the same layered substrate. CrystEngComm, 2013, 15, 6782.	2.6	12
203	CO2-facilitated transport performance of poly(ionic liquids) in supported liquid membranes. Journal of Materials Science, 2015, 50, 104-111.	3.7	12
204	Versatile construction of a hierarchical porous electrode and its application in electrochemical hydrogen production: a mini review. Materials Advances, 2021, 2, 1177-1189.	5.4	12
205	Superhydrophobic zeolitic imidazolate framework with suitable <scp>SOD</scp> cage for effective <scp>CH₄</scp> / <scp>N₂</scp> adsorptive separation in humid environments. AICHE Journal, 2022, 68, .	3.6	12
206	Kâ€Chabazite Zeolite Nanocrystal Aggregates for Highly Efficient Methane Separation. Angewandte Chemie - International Edition, 2022, 61, e202116850.	13.8	12
207	Molecular simulation of hydrogen storage in ion-exchanged Mazzite and Levyne zeolites. Computational and Theoretical Chemistry, 2012, 980, 1-6.	2.5	11
208	The synergistic effect of oxygen and water on the stability of the isostructural family of metal–organic frameworks [Cr ₃ (BTC) ₂] and [Cu ₃ (BTC) ₂]. Dalton Transactions, 2017, 46, 15573-15581.	3.3	11
209	Rapid and HF-free synthesis of MIL-100(Cr) via steam-assisted method. Materials Letters, 2019, 252, 286-288.	2.6	11
210	Enhancement effect of Mn doping on Co3O4 derived from Co-MOF for toluene catalytic oxidation. Chinese Journal of Chemical Engineering, 2022, 52, 1-9.	3.5	11
211	Cr-doped SnO2 microrods adhering nanoparticles for enhanced triethylamine sensing performance. Materials Letters, 2022, 312, 131684.	2.6	11
212	In situ growth Fe and V co-doped Ni3S2 for efficient oxygen evolution reaction at large current densities. International Journal of Hydrogen Energy, 2022, 47, 14422-14431.	7.1	11
213	Roughness Effect of Cu on Electrocatalytic CO ₂ Reduction towards C ₂ H ₄ . Chemistry - an Asian Journal, 2022, 17, .	3.3	10
214	Hydrogen storage in several metalâ€phosphate molecular sieves. AICHE Journal, 2008, 54, 3017-3025.	3.6	9
215	Reversible flexible structural changes in multidimensional MOFs by guest molecules (I2, NH3) and thermal stimulation. Journal of Solid State Chemistry, 2015, 226, 114-119.	2.9	9
216	Hierarchically Selfâ€Assembled Starâ€Shaped ZnO Microparticles for Electrochemical Sensing of Amines. Chemistry - A European Journal, 2016, 22, 8068-8073.	3.3	9

#	Article	IF	CITATIONS
217	NiFe2O4–Ni3S2 nanorod array/Ni foam composite catalyst indirectly controlled by Fe3+ immersion for an efficient oxygen evolution reaction. International Journal of Hydrogen Energy, 2021, 46, 14407-14417.	7.1	9
218	One-step synthesis of N, P co-doped porous carbon electrocatalyst for highly efficient nitrogen fixation. Nano Research, 2022, 15, 1779-1785.	10.4	9
219	Improved N2O capture performance of chromium terephthalate MIL-101 via substituent engineering. Journal of Solid State Chemistry, 2022, 309, 122951.	2.9	9
220	Linker micro-regulation of a Hofmann-based metal–organic framework for efficient propylene/propane separation. Inorganic Chemistry Frontiers, 2022, 9, 1082-1090.	6.0	9
221	Kâ€Chabazite Zeolite Nanocrystal Aggregates for Highly Efficient Methane Separation. Angewandte Chemie, 2022, 134, .	2.0	9
222	One-dimensional interpenetrated coordination polymers showing step gas sorption properties. CrystEngComm, 2013, 15, 1689.	2.6	8
223	Nanostructured iron(III) oxide catalyst electrodeposited from Fe(II) triflate for electrocatalytic water oxidation. International Journal of Hydrogen Energy, 2016, 41, 17193-17198.	7.1	8
224	Gas permeation properties of polymer membranes containing pendant tertiary amine groups. High Performance Polymers, 2016, 28, 1005-1014.	1.8	8
225	Synthesis and Gas-sensing Performance of Column-shaped Zinc Oxide Doped with-graphene. Materials Today: Proceedings, 2016, 3, 345-349.	1.8	8
226	Size-Controllable Strategy of ZnO Micro/Nanorods for Electrochemical Detection of H ₂ O ₂ . Journal of the Electrochemical Society, 2021, 168, 027507.	2.9	8
227	Energy efficient ethylene purification in a commercially viable ethane-selective MOF. Separation and Purification Technology, 2022, 282, 120126.	7.9	8
228	Engineering of Band Structure of Bismuth Selenide Ultrathin Nanosheets as Multifunctional Material for Photocatalytic Application. Advanced Materials Interfaces, 2022, 9, .	3.7	8
229	Ionothermal synthesis of two open-framework zirconium phosphates and their gas adsorption properties. Dalton Transactions, 2012, 41, 12915.	3.3	7
230	In-situ synthesis of Ag-Pi oxygen-evolving catalyst in phosphate environment for water splitting. International Journal of Hydrogen Energy, 2017, 42, 19935-19941.	7.1	7
231	Facile Preparation of Hierarchically Porous gâ€C ₃ N ₄ as Highâ€Performance Photocatalyst for Degradation of Methyl Violet Dye. ChemistrySelect, 2021, 6, 7130-7135.	1.5	7
232	Synthesis, structure and characterization of ZrPOF-DEA, a microporous zirconium phosphate framework material. Microporous and Mesoporous Materials, 2012, 164, 82-87.	4.4	6
233	Vapor-assisted preparation of Mn/Fe/Co/Zn–Cu bimetallic metal–organic frameworks based on octahedron micron crystals (PCN-6′). New Journal of Chemistry, 2019, 43, 6452-6456.	2.8	6
234	Enriching Low-Concentration Coalbed Methane Using a Hydrophobic Adsorbent under Humid Conditions. Industrial & Engineering Chemistry Research, 2021, 60, 12689-12697.	3.7	6

#	Article	IF	CITATIONS
235	A metal-free catalyst: sulfur-doped and sulfur nanoparticle-modified CMK-3 as an electrocatalyst for enhanced N ₂ -fixation. New Journal of Chemistry, 2020, 44, 20935-20939.	2.8	6
236	Ammonia Modification on UTSA-280 for C ₂ H ₄ /C ₂ H ₆ Separation. Acta Chimica Sinica, 2020, 78, 534.	1.4	6
237	Adsorption and separation of CH4/N2 by electrically neutral skeleton AlPO molecular sieves. Separation and Purification Technology, 2022, 286, 120497.	7.9	6
238	Controllable band structure of ZnO/g-C3N4 aggregation to enhance gas sensing for the dimethylamine detection. Sensors and Actuators Reports, 2022, 4, 100084.	4.4	6
239	Improving <scp>CH₄</scp> uptake and <scp>CH₄</scp> / <scp>N₂</scp> separation in pillar″ayered metal–organic frameworks using a regulating strategy of interlayer channels. AICHE Journal, 2022, 68, .	3.6	6
240	Tailoring Lewis Acid Properties of Metal–Organic Framework Nodes via Anion Post-Replacement for Gas Adsorption and Separation. ACS Sustainable Chemistry and Engineering, 2022, 10, 9359-9368.	6.7	6
241	Synthesis and properties of a zeolite LEV analogue from the system—Na2O–Al2O3–SiO2–N,N-dimethylpiperidine chloride–H2O. Catalysis Today, 2009, 148, 6-11.	4.4	5
242	Enhanced properties of solid solution (CeZr)O 2 modified with metal oxides for catalytic oxidation of low-concentration methane. Chinese Journal of Chemical Engineering, 2017, 25, 187-192.	3.5	5
243	Enhanced properties of Pd/CeO ₂ -nanorods modified with alkaline-earth metals for catalytic oxidation of low-concentration methane. RSC Advances, 2018, 8, 38641-38647.	3.6	5
244	Ultrafine tuning of the pore size in zeolite A for efficient propyne removal from propylene. Chinese Journal of Chemical Engineering, 2021, 37, 217-221.	3.5	5
245	Nitrogen rejection from low quality natural gas by pressure swing adsorption experiments and simulation using dynamic adsorption isotherms. Chinese Journal of Chemical Engineering, 2022, 42, 120-129.	3.5	5
246	Hydrogen Adsorption on Zeolite Na-MAZ and Li-MAZ Clusters. Wuli Huaxue Xuebao/ Acta Physico - Chimica Sinica, 2011, 27, 1647-1653.	4.9	5
247	Engineering biphasic hybrid phosphide nanowires as efficient electrocatalyst for hydrogen evolution reaction: Experimental and theoretical insights. International Journal of Hydrogen Energy, 2022, 47, 2926-2935.	7.1	5
248	Site trials of methane capture from low-concentration coalbed methane drainage wells using a mobile skid-mounted vacuum pressure swing adsorption system. Separation and Purification Technology, 2022, 295, 121271.	7.9	5
249	Hydrothermal Synthesis of Pure-Phase Copper Silicate Na2Cu2Si4O11·2H2O with Ammonia as Complexing Agent. European Journal of Inorganic Chemistry, 2011, 2011, 2112-2117.	2.0	4
250	RESEARCH ON THE ADSORPTION OF O2 IN METAL–ORGANIC FRAMEWORKS WITH OPEN MANGANESE(II) COORDINATION SITES. Functional Materials Letters, 2013, 06, 1350004.	1.2	4
251	The effect of barium-promoted for microsphere Ru/CeO ₂ catalysts in ammonia synthesis. Energy Sources, Part A: Recovery, Utilization and Environmental Effects, 2019, 41, 689-699.	2.3	4
252	Selective adsorption of propene over propane on Li-decorated poly (triazine imide). Green Energy and Environment, 2022, 7, 307-313.	8.7	4

#	Article	IF	CITATIONS
253	A dual-mode resonance Rayleigh scattering and colorimetric alkaline phosphatase assay based on <i>in situ</i> ascorbic acid-induced signal generation from manganese dioxide nanosheets. RSC Advances, 2020, 10, 31527-31534.	3.6	4
254	Hydrolysis of δ-Layered Sodium Disilicate in Ions Binding Process. Tenside, Surfactants, Detergents, 2006, 43, 130-136.	1.2	3
255	Cooperative structure-directing effects in the synthesis of a low-silica zeolite phillipsite analogue. Microporous and Mesoporous Materials, 2009, 121, 152-157.	4.4	3
256	Synthesis and characterization of [Cu(SiF ₆)(4,4′-bpy) ₂] with its H ₂ and CO ₂ adsorption. Journal of Coordination Chemistry, 2012, 65, 1645-1654.	2.2	3
257	A single precursor approach for ZIF synthesis: transformation of a new 1D [Zn(Im)(HIm)2(OAc)] structure to 3D Zn(Im)2 frameworks. CrystEngComm, 2015, 17, 3998-4005.	2.6	3
258	Size controlling preparation, adsorption and catalytic properties of silica microspheres. Chemical Research in Chinese Universities, 2016, 32, 843-847.	2.6	3
259	Stable titanium metal-organic framework with strong binding affinity for ethane removal. Chinese Journal of Chemical Engineering, 2022, 42, 35-41.	3.5	3
260	Bimetallic persulfide nanoflakes assembled by dealloying and sulfurization: a versatile electro-catalyst for overall water splitting and Zn–air batteries. Catalysis Science and Technology, 2022, 12, 497-508.	4.1	3
261	NC/Ni–Co3O4@Co1â^'xS Nanosheet Prepared from Metal Organic Framework for Highly Efficient Overall Water Splitting. Catalysis Letters, 2023, 153, 779-789.	2.6	3
262	The modulation of catalytic active site and support to construct high-efficiency ZnS/NC-X electrocatalyst for nitrogen reduction. Nano Research, 2022, 15, 7903-7909.	10.4	3
263	A phosphorus-doped potassium peroxyniobate electrocatalyst with enriched oxygen vacancies boosts electrocatalytic nitrogen reduction to ammonia. Dalton Transactions, 2022, 51, 11163-11168.	3.3	3
264	Synthesis of δLayered Sodium Disilicate with High Framework Stability. Tenside, Surfactants, Detergents, 2004, 41, 274-277.	1.2	2
265	The Synthesis and Properties of High Pure l´Layered Sodium Disilicate. Tenside, Surfactants, Detergents, 2007, 44, 34-39.	1.2	2
266	Interaction Between Al-δLayered Sodium Disilicate and Surfactant. Journal of Surfactants and Detergents, 2007, 10, 19-24.	2.1	2
267	A new 3D coordination polymer based on 2,6-dimethylpyridine-3,5-dicarboxylic acid and 4,4′-bipyridine mixed ligands. Inorganic Chemistry Communication, 2014, 48, 86-89.	3.9	2
268	Synthesis and Structural Characterization of a Two-Dimensional Magnesium Acetate, Mg7(OH)2(OAc)12(H2O)4·4H2O, a Precursor to Three-Dimensional Porous Magnesium Acetate. European Journal of Inorganic Chemistry, 2016, 2016, 3299-3304.	2.0	2
269	Nanostructured Fe(III) catalysts for water oxidation assembled with the aid of organic acid salt electrolytes. Applied Surface Science, 2016, 387, 1274-1280.	6.1	2
270	Facile synthesis of mesoporous Co3O4 nanoflowers for catalytic combustion of ventilation air methane. Chemical Research in Chinese Universities, 2017, 33, 965-970.	2.6	2

#	Article	IF	CITATIONS
271	In-situ ammonia-modulated silver oxide as efficient oxygen evolution catalyst in neutral organic carboxylate buffer. International Journal of Hydrogen Energy, 2018, 43, 14379-14387.	7.1	2
272	Shaping of metal–organic frameworks through a calcium alginate method towards ethylene/ethane separation. Chinese Journal of Chemical Engineering, 2022, 42, 17-24.	3.5	2
273	Boosting the Photoactivity of BiVO ₄ Photoanodes by a ZnCoFe‣DH Thin Layer for Water Oxidation. Chemistry - an Asian Journal, 2021, 16, 4095-4102.	3.3	2
274	Hydrolysis of α, β-Layered Sodium Disilicate in Ions Binding Process. Tenside, Surfactants, Detergents, 2008, 45, 6-12.	1.2	1
275	Boosting electrochemical nitrogen reduction to ammonia with high efficiency using a LiNb ₃ O ₈ electrocatalyst in neutral media. Dalton Transactions, 2022, 51, 1131-1136.	3.3	1
276	Amorphous CoV Phosphate Nanosheets as Efficient Oxygen Evolution Electrocatalyst. Chemistry - an Asian Journal, 2022, , .	3.3	1
277	Modulation and self-assembly of nanoparticles into bismuth molybdate nanosheets as highly efficient photocatalysts for ciprofloxacin degradation. Environmental Science: Nano, 2022, 9, 2979-2989.	4.3	1
278	Construction of a Porous Metal–Organic Framework with a High Density of Open Cr Sites for Record N ₂ /O ₂ Separation (Adv. Mater. 37/2021). Advanced Materials, 2021, 33, 2170291.	21.0	0
279	Investigation of the formation characteristics of methane hydrate in frozen porous media. Petroleum Science and Technology, 0, , 1-18.	1.5	0